PHYSICAL REVIEW D **87,** 012003 (2013)

Observation of η_c decay into $\Sigma^+\bar{\Sigma}^-$ and $\Xi^-\bar{\Xi}^+$ final states

M. Ablikim,[1] M. N. Achasov,[5] O. Albayrak,[3] D. J. Ambrose,[39] F. F. An,[1] Q. An,[40] J. Z. Bai,[1] Y. Ban,[27] J. Becker,[2] J. V. Bennett,[17] M. Bertani,[18a] J. M. Bian,[38] E. Boger,[20,*] O. Bondarenko,[21] I. Boyko,[20] R. A. Briere,[3] V. Bytev,[20] X. Cai,[1] O. Cakir,[35a] A. Calcaterra,[18a] G. F. Cao,[1] S. A. Cetin,[35b] J. F. Chang,[1] G. Chelkov,[20,*] G. Chen,[1] H. S. Chen,[1] J. C. Chen,[1] M. L. Chen,[1] S. J. Chen,[25] X. Chen,[27] Y. B. Chen,[1] H. P. Cheng,[14] Y. P. Chu,[1] F. Coccetti,[18a] D. Cronin-Hennessy,[38] H. L. Dai,[1] J. P. Dai,[1] D. Dedovich,[20] Z. Y. Deng,[1] A. Denig,[19] I. Denysenko,[20,†] M. Destefanis,[43a,43c] W. M. Ding,[29] Y. Ding,[23] L. Y. Dong,[1] M. Y. Dong,[1] S. X. Du,[46] J. Fang,[1] S. S. Fang,[1] L. Fava,[43b,43c] F. Feldbauer,[2] C. Q. Feng,[40] R. B. Ferroli,[18a] C. D. Fu,[1] J. L. Fu,[25] Y. Gao,[34] C. Geng,[40] K. Goetzen,[7] W. X. Gong,[1] W. Gradl,[19] M. Greco,[43a,43c] M. H. Gu,[1] Y. T. Gu,[9] Y. H. Guan,[6] A. Q. Guo,[26] L. B. Guo,[24] Y. P. Guo,[26] Y. L. Han,[1] F. A. Harris,[37] K. L. He,[1] M. He,[1] Z. Y. He,[26] T. Held,[2] Y. K. Heng,[1] Z. L. Hou,[1] H. M. Hu,[1] J. F. Hu,[36] T. Hu,[1] G. M. Huang,[15] G. S. Huang,[40] J. S. Huang,[12] X. T. Huang,[29] Y. P. Huang,[1] T. Hussain,[42] C. S. Ji,[40] Q. Ji,[1] Q. P. Ji,[26,‡] X. B. Ji,[1] X. L. Ji,[1] L. L. Jiang,[1] X. S. Jiang,[1] J. B. Jiao,[29] Z. Jiao,[14] D. P. Jin,[1] S. Jin,[1] F. F. Jing,[34] N. Kalantar-Nayestanaki,[21] M. Kavatsyuk,[21] M. Kornicer,[37] W. Kuehn,[36] W. Lai,[1] J. S. Lange,[36] C. H. Li,[1] Cheng Li,[40] Cui Li,[40] D. M. Li,[46] F. Li,[1] G. Li,[1] H. B. Li,[1] J. C. Li,[1] K. Li,[10] Lei Li,[1] Q. J. Li,[1] S. L. Li,[1] W. D. Li,[1] W. G. Li,[1] X. L. Li,[29] X. N. Li,[1] X. Q. Li,[26] X. R. Li,[28] Z. B. Li,[33] H. Liang,[40] Y. F. Liang,[31] Y. T. Liang,[36] G. R. Liao,[34] X. T. Liao,[1] B. J. Liu,[1] C. L. Liu,[3] C. X. Liu,[1] C. Y. Liu,[1] F. H. Liu,[30] Fang Liu,[1] Feng Liu,[15] H. Liu,[1] H. H. Liu,[13] H. M. Liu,[1] H. W. Liu,[1] J. P. Liu,[44] K. Y. Liu,[23] Kai Liu,[6] P. L. Liu,[29] Q. Liu,[6] S. B. Liu,[40] X. Liu,[22] Y. B. Liu,[26] Z. A. Liu,[1] Zhiqiang Liu,[1] Zhiqing Liu,[1] H. Loehner,[21] G. R. Lu,[12] H. J. Lu,[14] J. G. Lu,[1] Q. W. Lu,[30] X. R. Lu,[6] Y. P. Lu,[1] C. L. Luo,[24] M. X. Luo,[45] T. Luo,[37] X. L. Luo,[1] M. Lv,[1] C. L. Ma,[6] F. C. Ma,[23] H. L. Ma,[1] Q. M. Ma,[1] S. Ma,[1] T. Ma,[1] X. Y. Ma,[1] Y. Ma,[11] F. E. Maas,[11] M. Maggiora,[43a,43c] Q. A. Malik,[42] Y. J. Mao,[27] Z. P. Mao,[1] J. G. Messchendorp,[21] J. Min,[1] T. J. Min,[1] R. E. Mitchell,[17] X. H. Mo,[1] C. Morales Morales,[11] C. Motzko,[2] N. Yu. Muchnoi,[5] H. Muramatsu,[39] Y. Nefedov,[20] C. Nicholson,[6] I. B. Nikolaev,[5] Z. Ning,[1] S. L. Olsen,[28] Q. Ouyang,[1] S. Pacetti,[18b] J. W. Park,[28] M. Pelizaeus,[2] H. P. Peng,[40] K. Peters,[7] J. L. Ping,[24] R. G. Ping,[1] R. Poling,[38] E. Prencipe,[19] M. Qi,[25] S. Qian,[1] C. F. Qiao,[6] X. S. Qin,[1] Y. Qin,[27] Z. H. Qin,[1] J. F. Qiu,[1] K. H. Rashid,[42] G. Rong,[1] X. D. Ruan,[9] A. Sarantsev,[20,§] B. D. Schaefer,[17] J. Schulze,[2] M. Shao,[40] C. P. Shen,[37,‖] X. Y. Shen,[1] H. Y. Sheng,[1] M. R. Shepherd,[17] X. Y. Song,[1] S. Spataro,[43a,43c] B. Spruck,[36] D. H. Sun,[1] G. X. Sun,[1] J. F. Sun,[12] S. S. Sun,[1] Y. J. Sun,[40] Y. Z. Sun,[1] Z. J. Sun,[1] Z. T. Sun,[40] C. J. Tang,[31] X. Tang,[1] I. Tapan,[35c] E. H. Thorndike,[39] D. Toth,[38] M. Ullrich,[36] G. S. Varner,[37] B. Wang,[9] B. Q. Wang,[27] D. Wang,[27] D. Y. Wang,[27] K. Wang,[1] L. L. Wang,[1] L. S. Wang,[1] M. Wang,[29] P. Wang,[1] P. L. Wang,[1] Q. Wang,[1] Q. J. Wang,[1] S. G. Wang,[27] X. L. Wang,[40] Y. D. Wang,[40] Y. F. Wang,[1] Y. Q. Wang,[29] Z. Wang,[1] Z. G. Wang,[1] Z. Y. Wang,[1] D. H. Wei,[8] J. B. Wei,[27] P. Weidenkaff,[19] Q. G. Wen,[40] S. P. Wen,[1] M. Werner,[36] U. Wiedner,[2] L. H. Wu,[1] N. Wu,[1] S. X. Wu,[40] W. Wu,[26] Z. Wu,[1] L. G. Xia,[34] Z. J. Xiao,[24] Y. G. Xie,[1] Q. L. Xiu,[1] G. F. Xu,[1] G. M. Xu,[27] H. Xu,[1] Q. J. Xu,[10] X. P. Xu,[32] Z. R. Xu,[40] F. Xue,[15] Z. Xue,[1] L. Yan,[40] W. B. Yan,[40] Y. H. Yan,[16] H. X. Yang,[1] Y. Yang,[15] Y. X. Yang,[8] H. Ye,[1] M. Ye,[1] M. H. Ye,[4] B. X. Yu,[1] C. X. Yu,[26] H. W. Yu,[27] J. S. Yu,[22] S. P. Yu,[29] C. Z. Yuan,[1] Y. Yuan,[1] A. A. Zafar,[42] A. Zallo,[18a] Y. Zeng,[16] B. X. Zhang,[1] B. Y. Zhang,[1] C. Zhang,[25] C. C. Zhang,[1] D. H. Zhang,[1] H. H. Zhang,[33] H. Y. Zhang,[1] J. Q. Zhang,[1] J. W. Zhang,[1] J. Y. Zhang,[1] J. Z. Zhang,[1] S. H. Zhang,[1] X. J. Zhang,[1] X. Y. Zhang,[29] Y. Zhang,[1] Y. H. Zhang,[1] Y. S. Zhang,[9] Z. P. Zhang,[40] Z. Y. Zhang,[44] G. Zhao,[1] H. S. Zhao,[1] J. W. Zhao,[1] K. X. Zhao,[24] Lei Zhao,[40] Ling Zhao,[1] M. G. Zhao,[26] Q. Zhao,[1] Q. Z. Zhao,[9,¶] S. J. Zhao,[46] T. C. Zhao,[1] X. H. Zhao,[25] Y. B. Zhao,[1] Z. G. Zhao,[40] A. Zhemchugov,[20,*] B. Zheng,[41] J. P. Zheng,[1] Y. H. Zheng,[6] B. Zhong,[24] J. Zhong,[2] Z. Zhong,[9,¶] L. Zhou,[1] X. K. Zhou,[6] X. R. Zhou,[40] C. Zhu,[1] K. Zhu,[1] K. J. Zhu,[1] S. H. Zhu,[1] X. L. Zhu,[34] Y. C. Zhu,[40] Y. M. Zhu,[26] Y. S. Zhu,[1] Z. A. Zhu,[1] J. Zhuang,[1] B. S. Zou,[1] and J. H. Zou[1]

(BESIII Collaboration)

[1]*Institute of High Energy Physics, Beijing 100049, People's Republic of China*
[2]*Bochum Ruhr-University, 44780 Bochum, Germany*
[3]*Carnegie Mellon University, Pittsburgh, Pennsylvania 15213, USA*
[4]*China Center of Advanced Science and Technology, Beijing 100190, People's Republic of China*
[5]*G.I. Budker Institute of Nuclear Physics SB RAS (BINP), Novosibirsk 630090, Russia*
[6]*Graduate University of Chinese Academy of Sciences, Beijing 100049, People's Republic of China*
[7]*GSI Helmholtzcentre for Heavy Ion Research GmbH, D-64291 Darmstadt, Germany*
[8]*Guangxi Normal University, Guilin 541004, People's Republic of China*
[9]*GuangXi University, Nanning 530004, People's Republic of China*
[10]*Hangzhou Normal University, Hangzhou 310036, People's Republic of China*

[11]*Helmholtz Institute Mainz, J.J. Becherweg 45, D 55099 Mainz, Germany*
[12]*Henan Normal University, Xinxiang 453007, People's Republic of China*
[13]*Henan University of Science and Technology, Luoyang 471003, People's Republic of China*
[14]*Huangshan College, Huangshan 245000, People's Republic of China*
[15]*Huazhong Normal University, Wuhan 430079, People's Republic of China*
[16]*Hunan University, Changsha 410082, People's Republic of China*
[17]*Indiana University, Bloomington, Indiana 47405, USA*
[18a]*INFN Laboratori Nazionali di Frascati, Frascati, Italy*
[18b]*INFN and University of Perugia, I-06100 Perugia, Italy*
[19]*Johannes Gutenberg University of Mainz, Johann-Joachim-Becher-Weg 45, 55099 Mainz, Germany*
[20]*Joint Institute for Nuclear Research, 141980 Dubna, Russia*
[21]*KVI/University of Groningen, 9747 AA Groningen, The Netherlands*
[22]*Lanzhou University, Lanzhou 730000, People's Republic of China*
[23]*Liaoning University, Shenyang 110036, People's Republic of China*
[24]*Nanjing Normal University, Nanjing 210046, People's Republic of China*
[25]*Nanjing University, Nanjing 210093, People's Republic of China*
[26]*Nankai University, Tianjin 300071, People's Republic of China*
[27]*Peking University, Beijing 100871, People's Republic of China*
[28]*Seoul National University, Seoul 151-747, Korea*
[29]*Shandong University, Jinan 250100, People's Republic of China*
[30]*Shanxi University, Taiyuan 030006, People's Republic of China*
[31]*Sichuan University, Chengdu 610064, People's Republic of China*
[32]*Soochow University, Suzhou 215006, China*
[33]*Sun Yat-Sen University, Guangzhou 510275, People's Republic of China*
[34]*Tsinghua University, Beijing 100084, People's Republic of China*
[35a]*Ankara University, Ankara, Turkey*
[35b]*Dogus University, Istanbul, Turkey*
[35c]*Uludag University, Bursa, Turkey*
[36]*Universitaet Giessen, 35392 Giessen, Germany*
[37]*University of Hawaii, Honolulu, Hawaii 96822, USA*
[38]*University of Minnesota, Minneapolis, Minnesota 55455, USA*
[39]*University of Rochester, Rochester, New York 14627, USA*
[40]*University of Science and Technology of China, Hefei 230026, People's Republic of China*
[41]*University of South China, Hengyang 421001, People's Republic of China*
[42]*University of the Punjab, Lahore 54590, Pakistan*
[43a]*University of Turin, Turin, Italy*
[43b]*University of Eastern Piedmont, Alessandria, Italy*
[43c]*INFN, Turin, Italy*
[44]*Wuhan University, Wuhan 430072, People's Republic of China*
[45]*Zhejiang University, Hangzhou 310027, People's Republic of China*
[46]*Zhengzhou University, Zhengzhou 450001, People's Republic of China*

(Received 10 October 2012; published 3 January 2013)

Using a data sample of 2.25×10^8 J/ψ events collected with the BESIII detector, we present the first observation of the decays of η_c mesons to $\Sigma^+\bar{\Sigma}^-$ and $\Xi^-\bar{\Xi}^+$. The branching fractions are measured to be $(2.11 \pm 0.28_{\rm stat} \pm 0.18_{\rm syst} \pm 0.50_{\rm PDG}) \times 10^{-3}$ and $(0.89 \pm 0.16_{\rm stat} \pm 0.08_{\rm syst} \pm 0.21_{\rm PDG}) \times 10^{-3}$ for $\eta_c \to \Sigma^+\bar{\Sigma}^-$ and $\Xi^-\bar{\Xi}^+$, respectively. These branching fractions provide important information on the helicity selection rule in charmonium-decay processes.

DOI: 10.1103/PhysRevD.87.012003 PACS numbers: 13.25.Gv, 13.20.Gd, 14.40.Pq

I. INTRODUCTION

Experimental studies on exclusive charmonium decays play an important role in testing perturbative quantum chromodynamics (pQCD). In the Standard Model, the η_c meson is the lowest lying charmonium state in a 0^{-+} spin-parity configuration. Although the η_c cannot be produced directly from e^+e^- annihilations, it is produced copiously in radiative decays of J/ψ and ψ' [1]. The large J/ψ and

*Also at the Moscow Institute of Physics and Technology, Moscow, Russia.
†On leave from the Bogolyubov Institute for Theoretical Physics, Kiev, Ukraine.
‡Also at Nankai University, Tianjin 300071, China.
§Also at the PNPI, Gatchina, Russia.
‖Now at Nagoya University, Nagoya, Japan.
¶Also at Guangxi University, Nanning 530004, China.

ψ' data samples taken with the BESIII detector at the BEPCII provide an opportunity for a detailed study of η_c decays.

The complexity of QCD remains unsolved in the charmonium-mass region, and there are still many contradictions between pQCD calculations and experimental measurements. In particular, the pQCD helicity selection rule [2–4] is violated in many exclusive charmonium-decay processes, for example, the decay processes with meson pairs in the final state, like $J/\psi \to VP$, $\eta_c \to VV$, and $\chi_{c1} \to VV$, where V and P denote vector and pseudoscalar mesons. Other examples include decay processes with baryon antibaryon pairs in the final state, such as $\eta_c \to B_8\bar{B}_8$, and $\chi_{c0} \to B_8\bar{B}_8$, where $B_8\bar{B}_8$ denote the octet baryon antibaryon pairs. Many attempts have been made to understand these contradictions, such as by the quark-diquark model for the proton [5,6], constituent quark-mass corrections [7,8], mixing between the charmonium state and the glueball [9], and the quark pair creation model [10]. However, the measured branching fractions are not consistent with the predictions of any of these models.

In Refs. [11,12], intermediate meson loop (IML) transitions are proposed, where the long-distance interaction can evade the Okubo-Zweig-Iizuka rule and allow the violation of the pQCD helicity selection rule. Further calculations on the branching fractions of $\eta_c \to B_8\bar{B}_8$, $\chi_{c0} \to B_8\bar{B}_8$ and $h_c \to B_8\bar{B}_8$ based on charmed-meson loops were carried out [13], and the results agree with the measured branching fractions of $\eta_c \to p\bar{p}$ and $\eta_c \to \Lambda\bar{\Lambda}$. Using a sample of 2.25×10^8 J/ψ events [14] collected with the BESIII detector in 2009, we measure the branching fractions of $\eta_c \to \Sigma^+\bar{\Sigma}^-$ and $\eta_c \to \Xi^-\bar{\Xi}^+$ for the first time via the $J/\psi \to \gamma\eta_c$ radiative decay process.

II. DETECTOR AND MONTE CARLO SIMULATION

BEPCII [15] is a double-ring e^+e^- collider designed to provide a peak luminosity of 10^{33} $cm^{-2}s^{-1}$ at a center-of-mass energy of 3.77 GeV. The BESIII [15] detector has a geometrical acceptance of 93% of 4π and has four main components: (1) A small-cell, helium-based (40% He, 60% C_3H_8) main drift chamber with 43 layers providing an average single-hit resolution of 135 μm, charged-particle momentum resolution in a 1 T magnetic field of 0.5% at 1 GeV/c. (2) An electromagnetic calorimeter (EMC) consisting of 6240 CsI(Tl) crystals in a cylindrical structure (barrel) and two end caps. For 1 GeV photons, the energy resolution is 2.5% (5%) in the barrel (end caps), and the position resolution is 6 mm (9 mm) in the barrel (end caps). (3) A time-of-flight system consisting of 5-cm-thick plastic scintillators, with 176 detectors of 2.4 m length in two layers in the barrel and 96 fan-shaped detectors in the end caps. The barrel (end caps) time resolution of 80 ps (110 ps) provides 2σ K/π separation for momenta up to $\sim$1 GeV/c. (4) The muon system consists of 1000 m^2 of resistive plate chambers in 9 barrel and 8 end cap layers and provides 2-cm position resolution.

The optimization of the event selection and the estimate of backgrounds are performed using Monte Carlo (MC) simulated data. The GEANT4-based [16] simulation software BOOST [17] includes the geometry and the material description of the BESIII spectrometer, the detector response and digitization models, as well as the tracking of the detector running conditions and performances. The production of the J/ψ resonance is simulated by the MC event generator KKMC [18,19], while the decays are generated by EVTGEN [20] for the known decay modes with branching fractions set to world average values [1], and by LUNDCHARM [21] for the remaining unknown decays.

III. EVENT SELECTION

We select η_c mesons via the radiative decay $J/\psi \to \gamma\eta_c$ with its subsequent decay into $\Sigma^+\bar{\Sigma}^-$ and $\Xi^-\bar{\Xi}^+$. The Σ^+ candidates are reconstructed from the decay $\Sigma^+ \to p\pi^0$ with the π^0 decaying into a pair of photons; the Ξ^- candidates are reconstructed from the decays $\Xi^- \to \Lambda\pi^-$ and $\Lambda \to p\pi^-$. The antiparticle candidates, $\bar{\Sigma}^-$ and $\bar{\Xi}^+$, are reconstructed in a similar way but with the decay products changed to the corresponding antiparticles.

Tracks of charged particles in the polar-angle range $|\cos\theta| < 0.93$ are reconstructed from hits in the main drift chamber. The time-of-flight system and dE/dx information are combined to form particle identification (PID) confidence levels for the π, K and p hypotheses. Each track is assigned to the particle type that corresponds to the hypothesis with the highest confidence level. Photon candidates are reconstructed by clustering the energy deposited in the EMC crystals. The minimum energy requirement is 25 MeV for barrel showers ($|\cos\theta| < 0.80$) and 50 MeV for end cap showers ($0.86 < |\cos\theta| < 0.92$). Requirements on the EMC cluster timing are applied to suppress electronic noise and energy deposits unrelated to the event. Candidate π^0 mesons are reconstructed from pairs of photons with an invariant mass in the range $0.115\ \text{GeV}/c^2 < M(\gamma\gamma) < 0.155\ \text{GeV}/c^2$. The π^0 invariant-mass resolution is determined to be 4.2 MeV/c^2 by fitting the invariant-mass distribution of the $\gamma\gamma$ pairs from data after applying all the requirements except for the π^0-mass window, as shown in Fig. 1(a). In the fit, the π^0 signal is taken with a Gaussian form, and the background is described by a second-order Chebychev polynomial function.

For $J/\psi \to \gamma\eta_c \to \gamma\Sigma^+\bar{\Sigma}^-$, exactly one proton, one antiproton, at least five photons and at least two π^0 candidates from the combination of these photons are required. A four-constraint (4C) kinematic fit, based on momentum and energy conservation, is applied under the $J/\psi \to \gamma p\bar{p}\pi^0\pi^0$ hypothesis, and $\chi^2_{\text{4C}} < 30$ is required. For events with more than five photons or more than two π^0

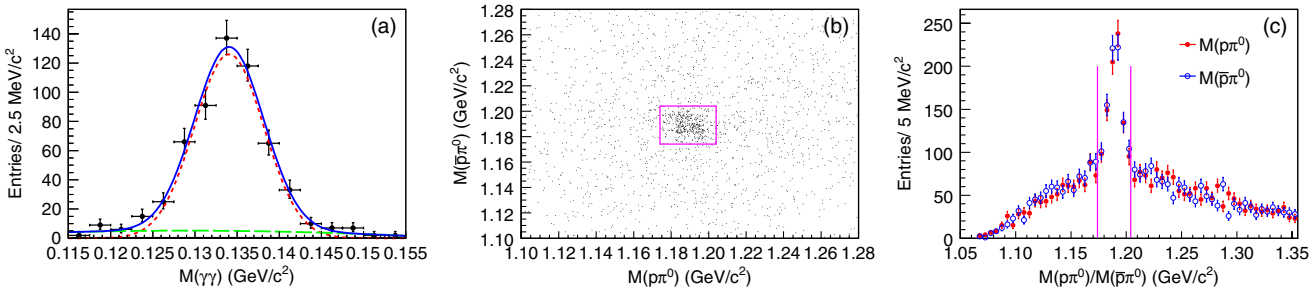

FIG. 1 (color online). (a) A fit to the invariant-mass distribution of $\gamma\gamma$ pairs after applying all the requirements except for the π^0-mass window. Dots with error bars are data, and the solid line is the total fit result. The signal is represented by the short-dashed line and the background by the long-dashed line. (b) A scatter plot for $M(\bar{p}\pi^0)$ versus $M(p\pi^0)$. (c) Invariant-mass distributions of $p\pi^0$ and $\bar{p}\pi^0$; solid dots with error bars are $M(p\pi^0)$, and the open circles with error bars are $M(\bar{p}\pi^0)$.

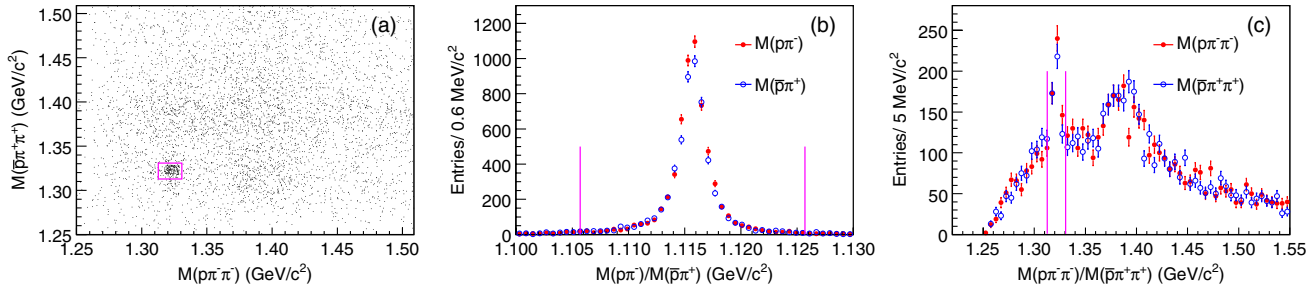

FIG. 2 (color online). (a) Scatter plot for $M(\bar{p}\pi^+\pi^+)$ versus $M(p\pi^-\pi^-)$. Invariant-mass distributions of (b) $p\pi^-$ and $\bar{p}\pi^+$, and (c) $p\pi^-\pi^-$ and $\bar{p}\pi^+\pi^+$. Solid dots with error bars are $M(p\pi^-)$ and $M(p\pi^-\pi^-)$, and open circles with error bars are $M(\bar{p}\pi^+)$ and $M(\bar{p}\pi^+\pi^+)$.

candidates, the combination with the minimum χ^2_{4C} is retained in the analysis. The events are also fitted to the $J/\psi \to p\bar{p}\pi^0\pi^0$ and $J/\psi \to \gamma\gamma p\bar{p}\pi^0\pi^0$ hypotheses. We require $\chi^2_{4C}(p\bar{p}\pi^0\pi^0) > 200$ and $\chi^2_{4C}(\gamma p\bar{p}\pi^0\pi^0) < \chi^2_{4C}(\gamma\gamma p\bar{p}\pi^0\pi^0)$. The p, $\bar{p}$ and the two π^0 candidates are combined to form the Σ^+ and $\bar{\Sigma}^-$ candidates by minimizing $(M_{p\pi^0_1} - M_{\Sigma^+})^2 + (M_{\bar{p}\pi^0_2} - M_{\bar{\Sigma}^-})^2$. Furthermore, the combined p, π^0 ($\bar{p}$, π^0) pair must have an invariant mass within 15 MeV/c^2 of the Σ^+ ($\bar{\Sigma}^-$) mass, as shown in Figs. 1(b) and 1(c).

For $J/\psi \to \gamma\eta_c \to \gamma\Xi^-\bar{\Xi}^+$, exactly one proton, one antiproton, two π^+s, two π^-s and at least one photon are required. A 4C kinematic fit is applied under the $J/\psi \to \gamma p\bar{p}\pi^+\pi^+\pi^-\pi^-$ hypothesis, and $\chi^2_{4C} < 90$ is required. For events with more than one photon candidate, only the combination with the minimum χ^2_{4C} is retained in the analysis. The events are also fitted to the $J/\psi \to p\bar{p}\pi^+\pi^+\pi^-\pi^-$ and $J/\psi \to \gamma\gamma p\bar{p}\pi^+\pi^+\pi^-\pi^-$ hypotheses. We require $\chi^2_{4C}(p\bar{p}\pi^+\pi^+\pi^-\pi^-) > 200$ and $\chi^2_{4C}(\gamma p\bar{p}\pi^+\pi^+\pi^-\pi^-) < \chi^2_{4C}(\gamma\gamma p\bar{p}\pi^+\pi^+\pi^-\pi^-)$.

To reconstruct the kinematical information of Λ and Ξ^-, vertex fits are applied to the charged tracks ($p\pi^-$ and $p\pi^-\pi^-$ for Λ and Ξ^-, respectively), with the requirement that all the tracks originated from the same decay point. Next, secondary vertex fits are applied to these reconstructed particles, with the requirement that their flight time is consistent with the one predicted from their final-state particles. The p, π^- ($\bar{p}$, π^+) combination with an invariant mass that is the closest to the Λ ($\bar{\Lambda}$) mass is chosen to form the Λ ($\bar{\Lambda}$). Furthermore, the mass difference must be within 10 MeV/c^2, as shown in Fig. 2(b). The p, π^-, π^- ($\bar{p}$, π^+, π^+) combination must have an invariant mass within 9 MeV/c^2 of the Ξ^- ($\bar{\Xi}^+$) mass, as shown in Figs. 2(a) and 2(c).

Figure 3 shows the invariant-mass distributions of $\Sigma^+\bar{\Sigma}^-$ and $\Xi^-\bar{\Xi}^+$ pairs after applying all the event selection criteria. A clear signature of an η_c resonance is observed.

IV. BACKGROUND STUDIES

The background can be classified into two categories: background from η_c decays which produces a peak within the η_c signal region, and background from J/ψ decays which gives a smooth distribution under the η_c resonance.

For $\eta_c \to \Sigma^+\bar{\Sigma}^-$, the potential peaking background channel is $\eta_c \to p\bar{p}\pi^0\pi^0$, which has not previously been measured. By requiring the invariant mass of any $p\pi^0$ combination to be outside a mass window of 50 MeV/c^2 centered at the Σ^+ mass and the $p\bar{p}\pi^0\pi^0$ invariant mass within 30 MeV/c^2 from the η_c mass, the number

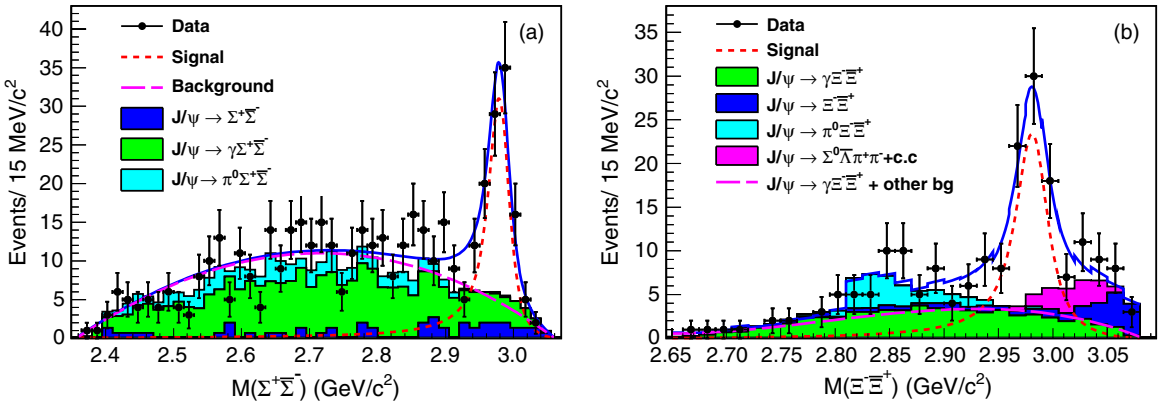

FIG. 3 (color online). Invariant-mass distributions of data and MC background channels together with the fitted curves for (a) $\Sigma^+\bar{\Sigma}^-$, and (b) $\Xi^-\bar{\Xi}^+$. Dots with error bars are data, and the histograms are the backgrounds from simulated J/ψ decays. Solid lines are the total fit results, signals are shown in short-dashed lines, and backgrounds are shown as long-dashed lines and shaded histograms.

of $\eta_c \to p\bar{p}\pi^0\pi^0$ events is obtained, and the branching fraction is determined to be $(5.0 \pm 0.6_{\rm stat}) \times 10^{-4}$, where the uncertainty is statistical only. Out of 5×10^5 $J/\psi \to \gamma\eta_c \to \gamma p\bar{p}\pi^0\pi^0$ MC simulated events, 193 events survive after applying the event selection criteria. Using the measured branching fraction, the background contribution from this process is estimated to be 0.7 events. For the background from J/ψ decays, the main sources are $J/\psi \to \Sigma^+\bar{\Sigma}^-$ and $J/\psi \to \pi^0\Sigma^+\bar{\Sigma}^-$, which have a fake photon or a photon from π^0 that escaped from detection, respectively, and $J/\psi \to \gamma\Sigma^+\bar{\Sigma}^-$, which is an irreducible background to the signal process. Using 5×10^5 MC simulated events for each channel and applying the event selection criteria to these MC samples, the background contributions are estimated by normalizing the number of the surviving events to the total number of J/ψ events. In the normalization, the branching fraction of $J/\psi \to \Sigma^+\bar{\Sigma}^-$ is taken from Ref. [1], and the branching fractions of $J/\psi \to \gamma\Sigma^+\bar{\Sigma}^-$ and $J/\psi \to \pi^0\Sigma^+\bar{\Sigma}^-$ are measured in this analysis. The branching fraction of $J/\psi \to \pi^0\Sigma^+\bar{\Sigma}^-$ is measured to be $(5.0 \pm 0.1_{\rm stat}) \times 10^{-4}$ using similar event selection criteria but with an additional photon and a π^0 reconstructed from the selected photons. The branching fraction of $J/\psi \to \gamma\Sigma^+\bar{\Sigma}^-$ is measured to be $(7.4 \pm 0.6_{\rm stat}) \times 10^{-5}$ with the same event selection criteria as was applied for the signal events, but without requiring that the $\Sigma^+\bar{\Sigma}^-$ system forms an η_c resonance and with a selection on the invariant mass of $2.4\ {\rm GeV}/c^2 < {\rm M}(\Sigma^+\bar{\Sigma}^-) < 2.8\ {\rm GeV}/c^2$. The total background is estimated to be 351 events in the entire mass region, as shown in Fig. 3(a). The total background shape is found to be smooth without an enhancement under the η_c resonance.

For $\eta_c \to \Xi^-\bar{\Xi}^+$, the potential peaking background channels are $\eta_c \to p\bar{p}\pi^+\pi^+\pi^-\pi^-$ and $\eta_c \to \Lambda\bar{\Lambda}\pi^+\pi^-$. Out of 2.5×10^5 simulated MC events for each channel, 2 and 21 events survived after applying the event selection criteria. The branching fractions of these two channels are determined to be $(6.7 \pm 1.0_{\rm stat}) \times 10^{-4}$ and $(6.3 \pm 0.4_{\rm stat}) \times 10^{-3}$, respectively, where the uncertainties are statistical only. The invariant-mass requirements for $\eta_c \to p\bar{p}\pi^+\pi^+\pi^-\pi^-$ are $|{\rm M}_{p\pi^-} - {\rm M}_\Lambda| > 20\ {\rm MeV}/c^2$ (no $p\pi^-$ combination consistent with a Λ), $|{\rm M}_{p\pi^-\pi^-} - {\rm M}_{\Xi^-}| > 25\ {\rm MeV}/c^2$ (no $p\pi^-\pi^-$ combination consistent with a Ξ^-), and $|{\rm M}_{p\bar{p}\pi^+\pi^+\pi^-\pi^-} - {\rm M}_{\eta_c}| < 30\ {\rm MeV}/c^2$; for $\eta_c \to \Lambda\bar{\Lambda}\pi^+\pi^-$, the only change is $|{\rm M}_{p\pi^-} - {\rm M}_\Lambda| < 20\ {\rm MeV}/c^2$. Using the measured branching fractions, the background contributions from the two peaking background channels are estimated to be 0.02 and 2 events to the signal after normalizing the number of the surviving events to the total number of the J/ψ events, respectively. The main background channels from J/ψ decays are $J/\psi \to \Xi^-\bar{\Xi}^+$ and $J/\psi \to \pi^0\Xi^-\bar{\Xi}^+$, which have one fake photon or one photon from the π^0 that escaped from detection, and $J/\psi \to \gamma\Xi^-\bar{\Xi}^+$, which is an irreducible background to the signal. Another background contribution from $J/\psi \to \Sigma^0\bar{\Lambda}\pi^+\pi^- \to \gamma\Lambda\bar{\Lambda}\pi^+\pi^-$ + c.c. is apparently seen from the invariant-mass distribution of $\gamma\Lambda$ pairs. To estimate the background contribution from the process $J/\psi \to \pi^0\Xi^-\bar{\Xi}^+$ including intermediate states, $J/\psi \to \pi^0\Xi^-\bar{\Xi}^+$ decays are reconstructed from data, and the signal yield is obtained in each ${\rm M}(\Xi^-\bar{\Xi}^+)$ mass bin. The selection criteria are similar to that for signal events but with an additional photon and a π^0 reconstructed from the selected photons. The relative efficiencies of the $\gamma\Xi^-\bar{\Xi}^+$ and $\pi^0\Xi^-\bar{\Xi}^+$ selection criteria are estimated in each ${\rm M}(\Xi^-\bar{\Xi}^+)$ mass bin using $J/\psi \to \pi^0\Xi^-\bar{\Xi}^+$ MC events. Combining this relative efficiency with the number of $J/\psi \to \pi^0\Xi^-\bar{\Xi}^+$ signal events in each ${\rm M}(\Xi^-\bar{\Xi}^+)$ mass bin, the number of $\pi^0\Xi^-\bar{\Xi}^+$ events that pass the $\gamma\Xi^-\bar{\Xi}^+$ selection is estimated. We generated 5×10^6 MC events for the channels $J/\psi \to \Xi^-\bar{\Xi}^+$ and

$J/\psi \to \Sigma^0\bar{\Lambda}\pi^+\pi^-$ + c.c. and 2.5×10^5 MC events for the channel of $J/\psi \to \gamma\Xi^-\bar{\Xi}^+$, and applied the event selection criteria to these MC samples. The contribution from each background process is estimated by normalizing the number of the surviving events to the total number of the J/ψ events. In the normalization, the branching fraction of $J/\psi \to \Xi^-\bar{\Xi}^+$ is taken from Ref. [1] and the branching fractions of $J/\psi \to \gamma\Xi^-\bar{\Xi}^+$ and $J/\psi \to \Sigma^0\bar{\Lambda}\pi^+\pi^-$ are measured in this analysis. The branching fraction of $J/\psi \to \Sigma^0\bar{\Lambda}\pi^+\pi^-$ is measured to be $(4.7 \pm 0.1_{\rm stat}) \times 10^{-4}$ by fitting the invariant-mass distribution of $\gamma\Lambda$ pairs. The branching fraction of $J/\psi \to \gamma\Xi^-\bar{\Xi}^+$ is measured to be $(1.8 \pm 0.5_{\rm stat}) \times 10^{-5}$ by excluding the $\Xi^-\bar{\Xi}^+$ system to form an η_c meson via the requirement $M(\Xi^-\bar{\Xi}^+) < 2.8$ GeV/c^2. The total background from J/ψ decays is estimated to be 116 events in the entire mass region, as shown in Fig. 3(b), and is smoothly distributed and no enhancement under the η_c resonance is observed.

V. SIGNAL EXTRACTIONS AND BRANCHING FRACTION CALCULATIONS

Signal yields are obtained from unbinned maximum likelihood fits to the invariant-mass distributions of $\Sigma^+\bar{\Sigma}^-$ and $\Xi^-\bar{\Xi}^+$ candidates. The probability density function (PDF) used in the fit is given by

$$F(m) = \sigma_{\rm res} \otimes (\varepsilon(m) \times E_\gamma^3 \times {\rm damping}(E_\gamma) \times {\rm BW}(m)) + {\rm BKG}(m),$$

where BW(m) and BKG(m) are the signal component described by the Breit-Wigner form and the background component, respectively; $\sigma_{\rm res}$ is the experimental resolution function and $\varepsilon(m)$ is the mass-dependent efficiency; E_γ^3 is the cube of the radiative photon energy and reflects the expected energy dependence of the magnetic-dipole (M1) matrix element; damping(E_γ) describes a function to damp the diverging tail caused by the E_γ^3 dependence and is given in the form of $\frac{E_0^2}{E_\gamma E_0 + (E_\gamma - E_0)^2}$ as used by KEDR [22], where E_0 is the peak energy of the transition photon.

The experimental resolution function is determined from a signal MC sample with the width of the η_c set to zero. A double Gaussian function is used for $\eta_c \to \Sigma^+\bar{\Sigma}^-$ and a single Gaussian function for $\eta_c \to \Xi^-\bar{\Xi}^+$. The mass-dependent efficiencies are determined from phase-space MC samples. The background component in the channel $\eta_c \to \Sigma^+\bar{\Sigma}^-$ is described by a third-order polynomial function. The background in the channel $\eta_c \to \Xi^-\bar{\Xi}^+$ is composed of four parts: (1) contributions of $J/\psi \to \Xi^-\bar{\Xi}^+$, $J/\psi \to \pi^0\Xi^-\bar{\Xi}^+$ and $J/\psi \to \Sigma^0\bar{\Lambda}\pi^+\pi^-$ + c.c., with shapes and normalizations fixed in the fit, (2) a third-order Chebychev polynomial function representing the phase-space background contribution from $J/\psi \to \gamma\Xi^-\bar{\Xi}^+$ and other possible processes, with parameters set free in the fit.

The signal detection efficiency is determined with MC simulated events by comparing the number of events after the event selection with the number of generated events. In the simulation, the decay $J/\psi \to \gamma\eta_c$ is generated using the helicity amplitude method [23], and the radiative photon follows the angular distribution of $1 + \cos^2(\theta)$, where θ is the polar angle of the radiative photon. The final-state baryons' angular distributions are assumed to be uniformly distributed in the rest frame of the η_c.

The fitted curves are shown in Fig. 3 for $\eta_c \to \Sigma^+\bar{\Sigma}^-$ and $\eta_c \to \Xi^-\bar{\Xi}^+$, where the mass and width of the η_c are fixed to the newly measured results from BESIII [24]. A possible interference between the η_c resonance amplitude and the nonresonant background is neglected. The observed number of events, $N_{\rm obs}$, are listed in Table I. The statistical significances of the signals are calculated using the changes in the log-likelihood values and the number of degrees of freedom (d.o.f) of the fits with and without the η_c signal assumptions. For $\eta_c \to \Sigma^+\bar{\Sigma}^-$, the change in $-ln(\mathcal{L})$ with Δ(d.o.f.) = 1 is 43.2, corresponding to a statistical significance of 9.3σ. For $\eta_c \to \Xi^-\bar{\Xi}^+$, the change in $-ln(\mathcal{L})$ with Δ(d.o.f.) = 1 is 20.2, corresponding to a statistical significance of 6.4σ. The branching fraction of $\eta_c \to \Sigma^+\bar{\Sigma}^-$ is calculated with

TABLE I. Branching fractions of $\eta_c \to \Sigma^+\bar{\Sigma}^-$ and $\eta_c \to \Xi^-\bar{\Xi}^+$ obtained from this analysis and the predictions based on IML. For the measured branching fractions, the first uncertainty is statistical, the second experimental systematic, and the third is from input branching fractions taken from Ref. [1].

	$\eta_c \to \Sigma^+\bar{\Sigma}^-$	$\eta_c \to \Xi^-\bar{\Xi}^+$
Statistical significance	9.3σ	6.4σ
$N_{\rm obs}$	112 ± 15	78 ± 14
$N_{\rm peaking}$	0.7	2.0
ε	5.3%	5.5%
Branching fraction (10^{-3})	$2.11 \pm 0.28 \pm 0.18 \pm 0.50$	$0.89 \pm 0.16 \pm 0.08 \pm 0.21$
Branching fraction based on IML [13] (10^{-3})	0.51–1.00	0.48–0.96

$$\mathcal{B}(\eta_c \to \Sigma^+\bar{\Sigma}^-) = \frac{N_{\rm obs} - N_{\rm peaking}}{N_{J/\psi} \times \mathcal{B}(J/\psi \to \gamma\eta_c) \times \mathcal{B}^2(\Sigma^+ \to p\pi^0) \times \mathcal{B}^2(\pi^0 \to \gamma\gamma) \times \varepsilon},$$

where $N_{\rm peaking}$ is the number of peaking background events determined from the background study, $N_{J/\psi}$ is the total number of J/ψ events, which is 2.25×10^8 with an uncertainty of 1.2% [14], $\mathcal{B}(J/\psi \to \gamma\eta_c)$, $\mathcal{B}(\Sigma^+ \to p\pi^0)$ and $\mathcal{B}(\pi^0 \to \gamma\gamma)$ are the branching fractions of $J/\psi \to \gamma\eta_c$, $\Sigma^+ \to p\pi^0$ and $\pi^0 \to \gamma\gamma$, respectively [1], and ε is the total detection efficiency. The branching fraction of $\eta_c \to \Xi^-\bar{\Xi}^+$ is calculated with:

$$\mathcal{B}(\eta_c \to \Xi^-\bar{\Xi}^+) = \frac{N_{\rm obs} - N_{\rm peaking}}{N_{J/\psi} \times \mathcal{B}(J/\psi \to \gamma\eta_c) \times \mathcal{B}^2(\Xi^- \to \Lambda\pi^-) \times \mathcal{B}^2(\Lambda \to p\pi^-) \times \varepsilon},$$

where $\mathcal{B}(\Xi^- \to \Lambda\pi^-)$ and $\mathcal{B}(\Lambda \to p\pi^-)$ are the branching fractions of $\Xi^- \to \Lambda\pi^-$ and $\Lambda \to p\pi^-$, respectively [1]. The results are summarized in Table I.

VI. SYSTEMATIC UNCERTAINTIES

The sources of systematic uncertainties for the two measurements are mainly from errors in the branching fractions of the known intermediate decay modes; the reconstruction and identification efficiencies of charged particles; the photon reconstruction; the π^0, Σ^+, Λ and Ξ^- selection; vertex fits and kinematic fits; the fitting to the invariant-mass distributions; event generators and the total number of the J/ψ events. The contributions are summarized in Table II.

The tracking and identification efficiency of protons from the Σ^+ decay is determined using the $J/\psi \to \Sigma^+\bar{\Lambda}\pi^-$ data sample. The recoiling mass distribution of $\bar{\Lambda}\pi^-$ pairs is fitted to obtain the Σ^+ signal yield, and the ratio between the yields with and without the requirement of tracking and identifying the proton from the Σ^+ decay is determined. The tracking and PID efficiency for simulated MC events agrees within 2.0% with that obtained from the experimental data for each charged track. Hence, adding the uncertainties of the proton and antiproton in quadrature, 2.8% is taken as the systematic uncertainty from reconstructing the final-state charged tracks and their identification for $\eta_c \to \Sigma^+\bar{\Sigma}^-$.

TABLE II. Systematic uncertainties (%) in the branching fraction measurements of $\eta_c \to \Sigma^+\bar{\Sigma}^-$ and $\eta_c \to \Xi^-\bar{\Xi}^+$.

Source	$\eta_c \to \Sigma^+\bar{\Sigma}^-$	$\eta_c \to \Xi^-\bar{\Xi}^+$
Tracking and PID	2.8	4.8
Photon reconstruction	5.0	1.0
π^0 selection	1.0	...
Σ^+-mass window	0.6	...
Λ-mass window	...	0.3
Ξ^--mass window	...	0.3
Vertex fits	...	0.5
Kinematic fits	4.3	3.8
Signal fitting	4.7	6.4
Event generators	0.4	2.8
Peaking background	0.3	1.3
$N_{J/\psi}$	1.2	1.2
Intermediate states	23.5	23.6
Total (BESIII)	8.7	9.5
Total	25.1	25.5

The tracking and PID efficiencies of p, $\bar{p}$, π^+ and π^- from Ξ^- and $\bar{\Xi}^+$ decays are determined from analyzing $J/\psi \to \Xi^-\bar{\Xi}^+ \to \Lambda\bar{\Lambda}\pi^+\pi^- \to p\bar{p}\pi^+\pi^+\pi^-\pi^-$ using a missing track method. Events are selected requiring all the tracks to be reconstructed except the one to be studied, and the invariant mass of the missing track predicted from the reconstructed tracks must be consistent with the invariant mass of the track to be studied. The tracking efficiency is then the fraction of the selected events with at least one additional track. The PID efficiency is obtained via the same missing track method. The tracking efficiency for MC simulated events is found to agree with that determined using data within 2.0% for each p, $\bar{p}$ track and 1.0% for each π^+ and π^- track. Adding the uncertainties from p, $\bar{p}$, π^+s and π^-s in quadrature, 4.0% is taken as the systematic uncertainty for the six charged track final states. The PID efficiency for MC simulated events agrees with that determined using the data within 1.0% for each p, 2.0% for each $\bar{p}$ and 0.5% for each π^+ and π^-, so 2.6% is taken as the systematic uncertainty for the $p\bar{p}\pi^+\pi^+\pi^-\pi^-$ identification by adding the uncertainties in quadrature.

The photon reconstruction efficiency is studied via three different methods: the missing photon method, the missing π^0 method and the π^0 decay angle method with $\psi' \to \pi^+\pi^- J/\psi \to \pi^+\pi^-\rho^0\pi^0$, $\psi' \to \pi^0\pi^0 J/\psi \to \pi^0\pi^0 l^+l^-$ and $J/\psi \to \rho^0\pi^0$ events, respectively. The efficiency difference between data and MC simulated events is within 1.0% for each photon [25]. Thus, 5.0% and 1.0% are taken as the systematic uncertainty due to photon reconstruction for $\eta_c \to \Sigma^+\bar{\Sigma}^-$ and $\eta_c \to \Xi^-\bar{\Xi}^+$, whose final states contain five photons and one photon, respectively.

The uncertainty of the π^0 selection is determined with the data sample $J/\psi \to \bar{\Sigma}^-\Lambda\pi^+ \to \pi^0 p\bar{p}\pi^+\pi^-$. The π^0-selection efficiency is determined from the change in the $\bar{\Sigma}^-$ signal yield from fitting the $\Lambda\pi^+$ recoiling mass distribution with and without the π^0-selection requirement.

The difference between beam data and MC simulated events on the π^0-selection efficiency is within 0.5% per π^0; hence 1.0% is taken as the systematic uncertainty from π^0 selection for $\eta_c \to \Sigma^+\bar{\Sigma}^-$.

Samples of $J/\psi \to \gamma K^{*+}\bar{K}^{*-} \to \gamma K^+K^-\pi^0\pi^0$, $J/\psi \to p\bar{p}\eta \to p\bar{p}\pi^0\pi^0\pi^0$ and $J/\psi \to \gamma\eta_c \to \gamma K^+K^-\pi^+\pi^+\pi^-\pi^-$ are selected to study the efficiency difference between beam data and simulated MC events in the kinematic fitting analysis for $\eta_c \to \Sigma^+\bar{\Sigma}^-$ and $\eta_c \to \Xi^-\bar{\Xi}^+$. In $\eta_c \to \Sigma^+\bar{\Sigma}^-$, the sample of $J/\psi \to \gamma K^{*+}\bar{K}^{*-} \to \gamma K^+K^-\pi^0\pi^0$ is selected to estimate the efficiency of the first two $\chi^2_{\rm 4C}$ requirements: $\chi^2_{\rm 4C}(p\bar{p}\pi^0\pi^0) > 200$ and $\chi^2_{\rm 4C}(\gamma p\bar{p}\pi^0\pi^0) < \chi^2_{\rm 4C}(\gamma\gamma p\bar{p}\pi^0\pi^0)$, and the efficiency of the $\chi^2_{\rm 4C}(\gamma p\bar{p}\pi^0\pi^0) < 30$ requirement is estimated by the change in the η signal yield from fitting the $p\bar{p}$ recoiling mass distribution from $J/\psi \to p\bar{p}\eta \to p\bar{p}\pi^0\pi^0\pi^0$ when the $\chi^2_{\rm 4C}$ of the $J/\psi \to p\bar{p}\pi^0\pi^0\pi^0$ hypothesis is less than 30. In $\eta_c \to \Xi^-\bar{\Xi}^+$, we select a clean $J/\psi \to \gamma\eta_c \to \gamma K^+K^-\pi^+\pi^+\pi^-\pi^-$ sample, plot the 4C kinematic fitting efficiency at different $\chi^2_{\rm 4C}$ requirements and obtain the efficiency for the requirements as described in the event selection section. The estimated systematic uncertainties are 4.3% and 3.8% from kinematic fitting for $\eta_c \to \Sigma^+\bar{\Sigma}^-$ and $\eta_c \to \Xi^-\bar{\Xi}^+$, respectively.

The uncertainty from the Σ^+-mass window requirement is estimated by selecting a sample of $J/\psi \to \Sigma^+\bar{\Sigma}^-$ events and by studying the efficiency difference between beam data and simulated MC events. An uncertainty of 0.6% is found.

The uncertainties from the vertex fits and from the Ξ^-, Λ-mass window requirements are estimated from a sample of $J/\psi \to \Xi^-\bar{\Xi}^+ \to \Lambda\bar{\Lambda}\pi^+\pi^- \to p\bar{p}\pi^+\pi^+\pi^-\pi^-$ events. The efficiency difference between beam data and simulated MC events is within 0.6%, 0.3% and 0.3% for the vertex fits, Ξ^- and Λ-mass window requirements, respectively.

Uncertainties from event generators are studied by comparing results with different models that were used for the generation of the signal events. The decays $\eta_c \to \Sigma^+\bar{\Sigma}^-$ and $\eta_c \to \Xi^-\bar{\Xi}^+$ are generated with another model using the helicity amplitude, and assuming that the baryons are uniformly distributed in the rest frame of η_c; the decays $\Sigma^+ \to p\pi^0$, $\Xi^- \to \Lambda\pi^-$ and $\Lambda \to p\pi^-$ are generated with another model, which takes parity violation effects into consideration. The efficiency differences are 0.4% and 2.8% for $\eta_c \to \Sigma^+\bar{\Sigma}^-$ and $\eta_c \to \Xi^-\bar{\Xi}^+$, respectively.

Uncertainties from fitting the invariant-mass distributions of $\Sigma^+\bar{\Sigma}^-$ and $\Xi^-\bar{\Xi}^+$ pairs are estimated by varying signal and background shapes and the corresponding fitting range. The mass and width of the η_c are varied by 1σ according to the new measurements from BESIII [24]; the damping function is changed from the form used by KEDR [22] to $e^{-\frac{E_\gamma^2}{8\beta^2}}$ with β fixed at 65 MeV, which was used by CLEO [26]; the MC signal shape is convoluted with a Gaussian with the width as a free parameter in the fit to study a possible uncertainty from the mass resolution determined from simulated MC events; the background shapes are varied either through the order of the polynomial or the normalization of fixed parts; the fitting range is varied to either a narrower or a wider one. Taking all the factors described above into account and by adding the uncertainties from each factor in quadrature, the uncertainties due to the fitting procedures are estimated to be 4.7% and 6.4% for $\eta_c \to \Sigma^+\bar{\Sigma}^-$ and $\eta_c \to \Xi^-\bar{\Xi}^+$, respectively.

The measured branching fractions of the peaking background channels have uncertainties around ~20–30%. The uncertainties from the number of peaking background events are estimated by assigning conservative estimates of 50% to the uncertainties of the measured branching fractions of $\eta_c \to p\bar{p}\pi^0\pi^0$, $\eta_c \to p\bar{p}\pi^+\pi^+\pi^-\pi^-$ and $\eta_c \to \Lambda\bar{\Lambda}\pi^+\pi^-$.

The total number of J/ψ events is determined from analyzing J/ψ inclusive hadronic decays, and the uncertainty is 1.2% [14].

Limited knowledge of the branching fractions, $\mathcal{B}(J/\psi \to \gamma\eta_c)$, $\mathcal{B}(\Sigma^+ \to p\pi^0)$, and $\mathcal{B}(\Lambda \to p\pi^-)$ contribute 23.5%, 0.6%, and 0.8% uncertainty to the measured branching fractions, respectively [1]. The first of these is the dominant source of systematic uncertainty, as indicated in Table II.

All the systematic uncertainties and their sources for the channels $\eta_c \to \Sigma^+\bar{\Sigma}^-$ and $\eta_c \to \Xi^-\bar{\Xi}^+$ are summarized in Table II. The quadratic sum of all the systematic uncertainties that solely stem from our experiment are 8.7% and 9.5% in the branching fraction measurements of $\eta_c \to \Sigma^+\bar{\Sigma}^-$ and $\eta_c \to \Xi^-\bar{\Xi}^+$, respectively. The total systematic uncertainty is about 25% for both measurements.

VII. SUMMARY

Using 2.25×10^8 J/ψ events collected with the BESIII detector, the decays $J/\psi \to \gamma\eta_c \to \gamma\Sigma^+\bar{\Sigma}^-$ and $J/\psi \to \gamma\eta_c \to \gamma\Xi^-\bar{\Xi}^+$ are observed for the first time, and their branching fractions are measured to be

$$\mathcal{B}(J/\psi \to \gamma\eta_c \to \gamma\Sigma^+\bar{\Sigma}^-) = (3.60 \pm 0.48 \pm 0.31) \times 10^{-5},$$
$$\mathcal{B}(J/\psi \to \gamma\eta_c \to \gamma\Xi^-\bar{\Xi}^+) = (1.51 \pm 0.27 \pm 0.14) \times 10^{-5}.$$

Using the known value of $\mathcal{B}(J/\psi \to \gamma\eta_c) = (1.7 \pm 0.4)\%$ [1], the branching fractions of $\eta_c \to \Sigma^+\bar{\Sigma}^-$ and $\eta_c \to \Xi^-\bar{\Xi}^+$ are obtained:

$$\mathcal{B}(\eta_c \to \Sigma^+\bar{\Sigma}^-) = (2.11 \pm 0.28 \pm 0.18 \pm 0.50) \times 10^{-3},$$
$$\mathcal{B}(\eta_c \to \Xi^-\bar{\Xi}^+) = (0.89 \pm 0.16 \pm 0.08 \pm 0.21) \times 10^{-3},$$

where the first uncertainties are statistical, the second systematic, and the third uncertainties are from the precision of the intermediate branching fractions.

Table I compares the results of our measurements with the predictions from charmed-meson loop calculations [13]. The measured branching fraction of $\eta_c \to \Sigma^+\bar{\Sigma}^-$ is larger than the prediction, while the measured branching fraction of $\eta_c \to \Xi^-\bar{\Xi}^+$ agrees with the prediction. Among the four η_c baryonic decays ($\eta_c \to p\bar{p}$, $\Lambda\bar{\Lambda}$, $\Sigma^+\bar{\Sigma}^-$, and $\Xi^-\bar{\Xi}^+$), only $\eta_c \to \Sigma^+\bar{\Sigma}^-$ disagrees with the prediction, which may indicate the violation of SU(3) symmetry.

The precision of the branching fraction measurements of $\eta_c \to \Sigma^+\bar{\Sigma}^-$ and $\eta_c \to \Xi^-\bar{\Xi}^+$ are limited by statistics, and the dominating systematic error stems from the uncertainty in the branching fraction of $J/\psi \to \gamma\eta_c$, which cannot be reduced without a thorough theoretical understanding of the η_c line shape in M1 transitions in the charmonium system.

ACKNOWLEDGMENTS

The BESIII Collaboration thanks the staff of BEPCII and the computing center for their hard efforts. This work is supported in part by the Ministry of Science and Technology of China under Contract No. 2009CB825200; National Natural Science Foundation of China (NSFC) under Contracts No. 10625524, No. 10821063, No. 10825524, No. 10835001, No. 10935007, No. 11125525, No. 10979038, No. 11079030, No. 11005109, No. 11179007, and No. 11275189; Joint Funds of the National Natural Science Foundation of China under Contracts No. 11079008 and No. 11179007; the Chinese Academy of Sciences (CAS) Large-Scale Scientific Facility Program; CAS under Contracts No. KJCX2-YW-N29 and No. KJCX2-YW-N45; 100 Talents Program of CAS; Research Fund for the Doctoral Program of Higher Education of China under Contract No. 20093402120022; Istituto Nazionale di Fisica Nucleare, Italy; Ministry of Development of Turkey under Contract No. DPT2006K-120470; U.S. Department of Energy under Contracts No. DE-FG02-04ER41291, No. DE-FG02-91ER40682, and No. DE-FG02-94ER40823; U.S. National Science Foundation; University of Groningen (RuG); the Helmholtzzentrum fuer Schwerionenforschung GmbH (GSI), Darmstadt; and WCU Program of National Research Foundation of Korea under Contract No. R32-2008-000-10155-0.

[1] J. Beringer *et al.* (Particle Data Group), Phys. Rev. D **86**, 010001 (2012).
[2] S. J. Brodsky and G. P. Lepage, Phys. Rev. D **24**, 2848 (1981).
[3] V. L. Chernyak and A. R. Zhitnitsky, Nucl. Phys. **B201**, 492 (1982).
[4] V. L. Chernyak and A. R. Zhitnitsky, Phys. Rep. **112**, 173 (1984).
[5] M. Anselmino, F. Caruso, S. Forte, and B. Pire, Phys. Rev. D **38**, 3516 (1988).
[6] M. Anselmino, F. Caruso, and S. Forte, Phys. Rev. D **44**, 1438 (1991).
[7] M. Anselmino, R. Cancelliere, and F. Murgia, Phys. Rev. D **46**, 5049 (1992).
[8] F. Murgia, Phys. Rev. D **54**, 3365 (1996).
[9] M. Anselmino, M. Genovese, and D. E. Kharzeev, Phys. Rev. D **50**, 595 (1994).
[10] R. G. Ping, B. S. Zou, and H. C. Chiang, Eur. Phys. J. A **23**, 129 (2005).
[11] Y. J. Zhang, G. Li, and Q. Zhao, Phys. Rev. Lett. **102**, 172001 (2009).
[12] X. H. Liu and Q. Zhao, Phys. Rev. D **81**, 014017 (2010).
[13] X. H. Liu and Q. Zhao, J. Phys. G **38**, 035007 (2011).
[14] M. Ablikim *et al.* (BESIII Collaboration), Chinese Phys. C **36**, 915 (2012).
[15] M. Ablikim *et al.* (BESIII Collaboration), Nucl. Instrum. Methods Phys. Res., Sect. A **614**, 345 (2010).
[16] S. Agostinelli *et al.* (GEANT4 Collaboration), Nucl. Instrum. Methods Phys. Res., Sect. A **506**, 250 (2003).
[17] Z. Y. Deng *et al.*, Chinese Phys. C **30**, 371 (2006).
[18] S. Jadach, B. F. L. Ward, and Z. Was, Comput. Phys. Commun. **130**, 260 (2000).
[19] S. Jadach, B. F. L. Ward, and Z. Was, Phys. Rev. D **63**, 113009 (2001).
[20] D. J. Lange, Nucl. Instrum. Methods Phys. Res., Sect. A **462**, 152 (2001); see also http://www.slac.stanford.edu/~lange/EvtGen/; R. G. Ping, Chinese Phys. C **32**, 599 (2008).
[21] J. C. Chen, G. Huang, X. Qi, D. Zhang, and Y. Zhu, Phys. Rev. D **62**, 034003 (2000).
[22] V. V. Anashin *et al.*, arXiv:1012.1694.
[23] C. Y. Pang and R. G. Ping, Commun. Theor. Phys. **51**, 1091 (2009).
[24] M. Ablikim *et al.* (BESIII Collaboration), Phys. Rev. Lett. **108**, 222002 (2012).
[25] M. Ablikim *et al.* (BESIII Collaboration), Phys. Rev. D **83**, 112005 (2011).
[26] R. E. Mitchell *et al.* (CLEO Collaboration), Phys. Rev. Lett. **102**, 011801 (2009).